

Arginine methylation regulates c-Myc-dependent transcription by altering promoter recruitment of the acetyltransferase p300

**Irina Tikhanovich<sup>1</sup>, Jie Zhao<sup>1</sup>, Brian Bridges<sup>2</sup>, Sean Kumer<sup>3</sup>, Ben Roberts<sup>2</sup> and Steven A. Weinman<sup>1,2</sup>**

<sup>1</sup>Department of Internal Medicine, <sup>2</sup>Liver Center, <sup>3</sup>Department of Surgery, University of Kansas Medical Center, Kansas City, KS 66160, U.S.A.

Running title: Arginine methylation regulates c-Myc

Address correspondence to: Steven A. Weinman, M.D., Ph.D. Department of Internal Medicine, University of Kansas Medical Center, 3901 Rainbow Blvd. Mail Stop 1018, Kansas City, KS 66160; Tel: 913-945-6945; Fax: 913-588-7501; E-mail: [sweinman@kumc.edu](mailto:sweinman@kumc.edu)

Keywords: post-translational modification, macrophage, monocyte, transcription factor, HDAC1, M2 macrophage

## ABSTRACT

Protein arginine methyltransferase 1 (PRMT1) is an essential gene controlling about 85% of total cellular arginine methylation in proteins. We have previously shown that PRMT1 is an important regulator of innate immune responses and that it is required for M2 macrophage differentiation. c-Myc is a transcription factor that is critical in regulating cell proliferation and also regulates the M2 transcriptional program in macrophages. Here, we sought to determine whether c-Myc in myeloid cells is regulated by PRMT1-dependent arginine methylation. We found that PRMT1 activity was necessary for c-Myc binding to the acetyltransferase p300. PRMT1 inhibition decreased p300 recruitment to c-Myc target promoters and increased histone deacetylase 1 (HDAC1) recruitment, thereby decreasing transcription at these sites. Moreover, PRMT1 inhibition blocked c-Myc-mediated induction of several of its target genes, including peroxisome proliferator-activated receptor gamma (PPAR $\gamma$ ) and mannose receptor C-type 1 (CD206), suggesting that PRMT1 is necessary for c-Myc function in M2 macrophage

differentiation. Of note, in primary human blood monocytes, p300-c-Myc binding was strongly correlated with PRMT1 expression, and in liver sections, PRMT1, c-Myc, and M2 macrophage levels were strongly correlated with each other. Both PRMT1 levels and M2 macrophage numbers were significantly lower in livers from individuals with a history of spontaneous bacterial peritonitis, known to have defective cellular immunity. In conclusion, our findings demonstrate that PRMT1 is an important regulator of c-Myc function in myeloid cells. PRMT1 loss in individuals with cirrhosis might contribute to their immune defects.

Protein arginine methylation is a common posttranslational modification that plays a role in multiple pathways, including cell cycle control, RNA processing and DNA replication (1). PRMT1 is responsible for about 85% of total cellular arginine methylation (2). It methylates both histone and non-histone proteins, however many protein targets are not yet defined (3). Arginine methylation impacts gene transcription and splicing as well as upstream signal transduction including a number of innate immunity pathways (4).

Abnormal function of PRMT1 is closely associated with several types of cancer and cardiovascular disease suggesting a relationship between arginine methylation and both inflammation and cell growth control.

c-Myc is a protooncogene that is associated with tumor development and is involved in pathways important for cell growth and survival (5,6). c-Myc, together with its partner Max can induce expression of large number of genes (5). In addition, c-Myc can suppress the expression of genes through its binding to Miz1(5,7). More recently, a number of studies have reported a key role of c-Myc in myeloid cell survival and function (8-10).

We recently discovered that the protein arginine methyltransferase PRMT1 reversibly regulates a broad array of TLR-dependent innate immune signaling pathways via methylation of TRAF6 (11) and regulation of PPAR $\gamma$  expression (12). This latter function is necessary for survival in in vivo models of septic shock (12) but the detailed mechanism of PRMT1 dependent PPAR $\gamma$  regulation was not studied. PPAR $\gamma$  is induced during M2 macrophage differentiation and is regulated by number of transcription factors including STAT6, IRF4 and c-Myc (10,13-17).

In this study we examined the role of PRMT1 dependent methylation in c-Myc dependent gene transcription. We found that c-Myc arginine methylation was necessary to allow it to recruit the histone acetyltransferase p300 to promoters. Arginine methylation served to determine the balance between c-Myc's transcriptional inhibitory and activating functions. PRMT1 activity was necessary for c-Myc's ability to induce M2 genes including PPAR $\gamma$  and MRC1. We found that M2 macrophage numbers in human livers correlated with both c-Myc and PRMT1 expression. This PRMT1-c-Myc axis thus appears to be a factor altering innate immune responses both in vitro and in vivo.

## RESULTS

### Arginine methylation is required for c-Myc-p300 interaction

We recently discovered that the protein arginine methyltransferase PRMT1 regulates innate immune signaling pathways in monocytes and macrophages, via regulation of expression of a number of target genes (11,12). However, the detailed mechanism of PRMT1-dependent regulation of gene expression is not entirely clear. Some studies suggest that PRMT1 is recruited to the promoters of target genes by a transcription factor where it then modifies both histones and transcription factors to facilitate gene expression (18,19). c-Myc is an important transcription factor regulating myeloid cell functions (8-10). Previous studies on c-Myc and N-Myc regulation by PRMT1 suggested that PRMT1 can regulate Myc gene expression (20,21) and function (21).

In order to determine how PRMT1 might affect c-Myc we analyzed c-Myc expression in THP-1 cells by immunofluorescence in the presence of the PRMT1 inhibitor AMI-1. AMI-1 treatment did not change the expression or subcellular localization of c-Myc (Fig. 1A). Next we examined the effect of AMI-1 on the binding of c-Myc to the transcriptional cofactors Max, Miz-1, p300 and HDAC1. We found that the c-Myc-p300 interaction in THP-1 cells was reduced by AMI-1 (Fig. 1B, C). We also observed a decrease in c-Myc-Max binding but there was no effect of AMI-1 on the c-Myc-HDAC1 interaction (Fig. 1B). Figure 1D shows detection of the PRMT1-c-Myc interaction using proximity ligation assay (PLA), seen as brown/red dots throughout the cell. Similar to the immunoprecipitation results, PLA signal for c-Myc-p300 and c-Myc-Max interactions was abolished by AMI-1 (Fig. 1E). The c-Myc-Miz1 PLA signal was not changed. Additionally, we found that c-Myc-p300 and

c-Myc-Max but not c-Myc-HDAC1 interactions were reduced in peritoneal macrophages isolated from PRMT1 myeloid KO mice (Fig. 1F).

These results suggest that arginine methylation is required for c-Myc/p300 binding. To determine if c-Myc is a target of PRMT1 we purified c-Myc protein and analyzed it by mass-spectrometry. We found that c-Myc is arginine methylated on two residues located in the C-terminal portion of its transactivation domain involved in c-Myc-p300 interaction (Fig. 2A, B).

To determine if PRMT1 levels actually correlate with the cMyc-p300 interaction in primary monocytes and confirm the relevance of the above findings to humans, we measured p300-c-Myc binding in human primary monocytes using a modified sandwich ELISA assay. We observed wide variations in PRMT1 levels between individuals with a significant correlation between p300-c-Myc binding and PRMT1 expression in these samples (Fig. 2C).

### **Arginine methylation is required for c-Myc-p300 interaction at target gene promoters**

Next we tested the effects of PRMT1 inhibition on p300 binding to c-Myc target gene promoters. Loss of methylation did not affect c-Myc promoter binding to its target genes but decreased p300 and to a lesser extent Max recruitment to cyclinB1 and CDK4 promoters as evidenced by p300 ChIP (Fig. 3A). That the loss of p300 promoter binding was due to its failure to bind c-Myc was shown by ChIP-re ChIP experiments with c-Myc ChIP followed by p300 re-ChIP (Fig. 3B). Reduced binding of p300 might allow for binding of other factors such as HDAC1, similarly to the previously described switch from Myc-p300 to Myc-HDAC1 at SNAIL, ZEB1 and ZEB2 promoters (22). Indeed, AMI-1 did increase HDAC1 binding at the c-

Myc target gene promoters cyclin B1 and CDK4 (Fig. 3A,B). This combination of the decrease in p300 and increase in HDAC1 recruitment resulted in reduced levels of histone H3K27 acetylation (H3ac) at these promoters (Fig. 3A). Similarly, c-Myc also bound to PPAR $\gamma$ , STAT6 and MRC1 promoters, consistent with previously published data (10) (Fig. 3C). We also detected significant ability of AMI-1 to reduce c-Myc-p300 recruitment to the PPAR $\gamma$  and MRC1 promoters but not to the STAT6 promoter (Fig. 3C, D).

### **Arginine methylation regulates c-Myc transcriptional activity**

To assess the effect of methylation-dependent changes in p300/HDAC1 recruitment and histone acetylation on c-Myc target gene mRNA expression we performed a series of experiments in which we measured target gene mRNA after overexpression of cMyc before and after inhibition of methylation with AMI-1. Upon initially characterizing the effects of c-Myc overexpression in this system, we unexpectedly observed that overexpression of c-Myc led to a decrease in PRMT1 expression both at the protein and mRNA level (Fig. 4A). This ability of c-Myc to suppress PRMT1 complicated the use of c-Myc overexpression as a tool to determine how c-Myc effects are modulated by its own arginine methylation.

To overcome this problem we compared the effects of the methylation inhibitor on c-Myc overexpression driven gene expression with and without the simultaneous overexpression of PRMT1. Fig 4B demonstrates these results. c-Myc was overexpressed in either untreated THP-1 cells or cells treated with AMI-1. c-Myc overexpression stimulated the transcription of cyclinB1, CDK4 and the PPAR $\gamma$  target gene CD209 (Fig. 4B), but the magnitude of this stimulation was small. The combination of PRMT1 and c-Myc co-

expression resulted in a significantly higher increase in mRNA levels for all genes except STAT6. Since CD209 is not a direct target of c-Myc, the effect on its expression could be due to PPAR $\gamma$  upregulation. In all cases this stimulation was mediated by PRMT1 enzymatic activity since addition of AMI-1 abolished the effect (Fig. 4B). Since c-Myc regulates M2 macrophage differentiation through PPAR $\gamma$  and other M2 gene expression including MRC1 (10), we measured expression of MRC1 in THP-1 macrophages expressing either c-Myc, PRMT1 or both in the presence or absence of the PRMT1 inhibitor AMI-1 (Fig. 4C). We found that c-Myc overexpression induced MRC-1 to a higher level in the presence of PRMT1 overexpression, and induction was abolished in the presence of the methylation inhibitor (Fig. 4C).

**An R299K\_R346K mutant c-Myc is deficient in the ability to recruit p300 to CyclinB1 and CDK4 promoters.**

To verify the functional role of c-Myc arginine methylation at R299 and R346 we mutated both residues to lysine and tested single and double mutants for function. First, we tested whether these mutations abolish c-Myc arginine methylation as measured by PLA. Fig. 5A shows that there were no effects of these mutations on the PLA signal resulting from proximity of c-Myc and Max or c-Myc and HDAC1, but did show reduced p300 binding when both sites were mutated (Fig. 5A).

Next we tested the ability of the mutants to recruit p300 to c-Myc target promoters. All three mutants showed normal binding to cyclinB1 and CDK4 promoters (Fig. 5B). However, CHIP-re-CHIP experiments showed that unlike the wild-type protein, the R299K\_R346K double mutant lost the ability to recruit p300 to both promoter sites. Consistent with this result, double mutant c-Myc was less efficient in inducing the

transcription of cyclinB1 and CDK4 mRNA especially in the presence of PRMT1 (Fig. 5C), although the mutation did not abolish the ability of PRMT1 to induce those genes completely. Taken together these data suggest that PRMT1-dependent methylation of c-Myc at R299 and R346 controls both recruitment of p300 to c-Myc target gene promoters and expression of these genes.

**PRMT1 is downregulated in liver cells from patients with decompensated cirrhosis.**

Patients with cirrhosis have a number of well-known abnormalities in their response to bacterial infections (23). Spontaneous bacterial peritonitis (SBP) is an extreme example of an infectious complication that results, in part, from the immune system defects in advanced cirrhosis patients. To evaluate whether PRMT1 dependent regulation correlates with innate immune defects in patients with liver disease we examined PRMT1 levels in livers of patients with cirrhosis with or without history of SBP. PRMT1 protein levels were significantly decreased in both hepatocytes and non-parenchymal cells from patients with a history of SBP (Fig. 6A). Reduced PRMT1 expression correlated with reduced numbers of MRC1 positive M2 macrophages in those livers (Fig. 6B,C). Co-staining with anti-PRMT1 and anti-CD206 (MRC1) antibodies revealed that majority of M2 macrophages are PRMT1 positive. Co-staining with anti-c-Myc and anti-MRC1 antibodies showed that high levels of c-Myc expression in the cirrhotic livers are found only in M2 macrophages (MRC1 positive cells) (Fig. 6D). Figure 6E shows that number of M2 macrophages correlated with both PRMT1 expression and c-Myc expression. Moreover, we found that M2 macrophage number is significantly higher when both PRMT1 and c-Myc are high ('high high' group) compared to the situation when either of them is low (Fig. 6F). Taken together these data suggest that in human liver



PRMT1 and c-Myc cooperatively regulate M2 macrophage numbers.

## DISCUSSION

The work presented in this study identified a novel interaction between c-Myc and PRMT1 in which arginine methylation is necessary for c-Myc's ability to recruit p300 to target gene promoters and serve as a transcriptional activator (Fig. 7). Recent studies have observed that c-Myc posttranslational modifications can serve as to switch c-Myc between positive and negative regulation of gene promoters (24). Our results suggest that arginine methylation may be such an activation/inactivation switch. This effect is important at a number of gene promoters and is required for M2 macrophage differentiation, possibly as a result of its regulation of the expression of PPAR $\gamma$ .

We found that c-Myc is arginine methylated at R299 and R364, and these sites control c-Myc binding to p300. Mutation of those sites to lysine abolishes p300 binding without affecting binding to other co-factors such as HDAC1 and Max. Interestingly binding c-Myc to Max is also inhibited by the PRMT1 inhibitor AMI-1 suggesting that this binding is controlled by other arginine methylation sites on c-Myc or possibly Max itself that are not identified in this study.

Regulation of gene transcription is often mediated by recruitment of various chromatin remodeling enzymes to promoter sites. c-Myc recruits several of these enzymes through its transactivation domain including p300 and p400 (part of acetyltransferase complexes), SKP2 (a histone ubiquitination enzyme), HDAC1 (a histone deacetylase), DNMT1 and others (5). We showed that recruitment of two of those factors, p300 and HDAC1 are regulated by PRMT1. Previous studies have also reported PRMT1-mediated regulation of

p300 recruitment by other transcription factors such as HNF-4 alpha (18), p53 (19) as well as others (25). The mechanism of this regulation involved both arginine methylation of the transcription factor itself together with methylation of histones at the target gene promoters. We propose that a similar mechanism is regulating c-Myc function. However, we only observed partial inhibition of gene activation in c-Myc methylation deficient mutants suggesting that other factors such as histone methylation or additional methylation sites might also play a role.

Previously we showed that PRMT1 expression is inhibited in livers of patients with cirrhosis (26). However, the reason for low PRMT1 levels is still unclear. We have observed that overexpression of c-Myc, by itself is able to decrease expression of PRMT1 (Fig. 4A). Since reduced PRMT1 could subsequently decrease c-Myc methylation, the possibility of a positive feedback loop exists where an increase in c-Myc could perpetuate a decrease in PRMT1 expression. Whether a mechanism of this nature is occurring in cirrhosis with SBP is uncertain.

In this study we further showed that PRMT1 controls macrophage phenotype in livers of patients with cirrhosis likely through its regulation of c-Myc transcriptional activity at M2 gene promoters. In patients with cirrhosis, particularly those most immunocompromised with a history of spontaneous bacterial peritonitis (SBP), the levels of PRMT1 protein in liver tissue were extremely low and this correlated with low M2 macrophage numbers. Lack of M2 macrophage differentiation can result in enhanced susceptibility to bacterial infections. Thus PRMT1 deficiency can contribute to immune defects seen in those patients.

In addition to its association with M2 differentiation, c-Myc activation in myeloid and other cells has been associated with development and progression of cancer

(10,27-30). Since PRMT1 is necessary for c-Myc gene activation, its inhibition in this regard might be beneficial. It is known that overexpression of PRMT1 is associated with number of cancers and PRMT1 promotes cancer cell proliferation (1,4). The data presented in this study suggests that the inhibition of PRMT1 in cirrhosis might play a beneficial or tumor suppressor role due to inhibition of c-Myc dependent gene activation. A full understanding of the role of c-Myc-PRMT1 interactions in tumor cell growth will require further studies.

In summary, this study has demonstrated a novel mechanism by which arginine methylation via the methyltransferase PRMT1 regulates the activity of c-Myc. Low PRMT1 is a characteristic of multiple cell types derived from patients with advanced, decompensated cirrhosis and further understanding of these interactions could lead to new therapeutic approaches to deal with immune defects and cell growth abnormalities in these patients.

## MATERIALS AND METHODS

### Antibodies used

#### Primary antibodies:

Anti-PRMT1 (F339), Acetyl-Histone H3 (Lys27) (D5E4) and HDAC1 (10E2) Mouse monoclonal Antibodies were from Cell Signaling. Anti-Lamin B (C20), ChIP grade anti-Max (C-17), anti-p300 and anti-Miz1 (H-190) and monoclonal anti-MRC1 anti- $\beta$ -actin were from Santa Cruz. Anti-mono and dimethyl arginine (clone 7E6), rabbit Anti-PRMT1 antibody (against aa 300-361), ChIP grade Anti-Max antibody [73C5a], mouse ChIP grade Anti-c-Myc antibody [9E11] and rabbit Anti-c-Myc antibody [Y69] were from Abcam. Anti-asymmetric-dimethyl-arginine antibodies were from ActiveMotif. Mouse

anti-  $\beta$ -actin, mouse Monoclonal Anti-PRMT1 antibody clone 171 (against aa 1-361) and anti-Flag (M2) antibodies were from Sigma-Aldrich, Saint Louis, MO. Anti-GAPDH was from Ambion.

#### Secondary antibodies:

IRDye 800CW goat anti-mouse IgG and IRDye 680RD goat anti-rabbit IgG were from Li-COR. General HRP-conjugated secondary antibodies were from Southern Biotechnology Associates (Birmingham, AL).

#### Cell culture

THP-1 cells were from InvivoGen and were maintained according to recommended procedures. AMI-1 was obtained from EMD4 Biosciences and used at 10  $\mu$ M for 16-24h prior to harvest. Cells were transfected using Lipofectamine LTX transfection reagent (Invitrogen) according to the manufacturer's protocol.

#### Isolation of mouse peritoneal macrophages

Myeloid specific PRMT1 knockout mice were described previously (12). Primary peritoneal macrophages were isolated from PRMT1fl/fl LysM Cre or PRMT fl/fl wild type littermates as described previously (31). 8-10 week old mice were killed by CO<sub>2</sub> asphyxiation. Briefly, 10 ml of sterile PBS was injected into the caudal half of the peritoneal cavity using a 25-gage needle (beveled side up), following by gentle shaking the entire body for 10 seconds. Saline containing resident peritoneal cells was collected and cells were plated on uncoated tissue culture plates and incubated for 60 minutes at 37°C. Nonadherent cells were removed by washing five times with warm PBS. Macrophages were maintained in RPMI medium (Invitrogen) containing 10% FBS

#### Vectors

pcDNA3-cmyc plasmid was provided by Wafik El-Deiry via Addgene (Addgene plasmid 16011). pCMV6-PRMT1 was from Origene. The Myc point mutations and C-terminal Flag-tag were generated by site directed mutagenesis (Q5® Site-Directed Mutagenesis Kit, NEB).

### Human specimens

De-identified human liver specimens from liver explants were obtained from the Liver Center Tissue Bank at the University of Kansas Medical Center. All studies using human tissue samples were approved by the Human Subjects Committee of the University of Kansas Medical Center.

Peripheral blood mononuclear cells were isolated from PBMC fraction using MACS beads (human CD14) (Miltenyi Biotec, 130-050-201) according to manufacturer's instructions.

### LC/MS analysis

Ten 15 cm dishes of THP-1 cells were seeded at  $1 \times 10^7$  cells per dish and were transiently transfected with 30 µg of Myc-Flag plasmid per dish. Cells were harvested 48 hours post-transfection. Myc-Flag was purified using Flag-purification kit from Sigma according to the manufacturer's instructions. Identification of methyl-Arg and acetyl-Lys on Myc was done using in-gel digestion with endoproteinase trypsin, LC-MS/MS and database searching were performed by MS Bioworks LLC, 3950 Varsity Drive, Ann Arbor, MI.

### Real Time PCR

RNA was extracted from cultured cells using the RNeasy Mini Kit (Qiagen). cDNA was generated using the RNA reverse transcription kit (Applied Biosystems, Cat.No 4368814). Quantitative real time RT-PCR was performed in a CFX96 Real time system (Bio-Rad) using specific sense and antisense primers combined with iQ SYBR Green Supermix (Bio-Rad) for

40 amplification cycles: 5 s at 95 °C, 10 s at 57 °C, 30 s at 72 °C. Primers were as follows:

Actin B, gtgctcgatggggtacttcag, tgatgggtgggcatgggtcag; PRMT1, caggcggaagcagtgagaa, gatgccaaagtgtgcgtagg; Cyclin B1, tctggataatggatgaatggaca, cgatgtggcatacttgttcttg; CDK4, acgggtgtaagtgccatctg, tgggtcgggtgcctatggga; STAT6, atggggcaacagaaaagatg, gcacagaagacagcagcaag; CD209, tcaagcagtattggaacagagga, caggaggctgcggacttttt; PPARγ, ggctccataaagtcaccaa, gctgtgcaggagatcacaga

### Chromatin immunoprecipitation (ChIP) assay

Chromatin immunoprecipitation was performed as described previously (12,32). THP-1 cells ( $1.5 \times 10^7$ ) were cross-linked by the addition of 1% formaldehyde for 10 minutes. Cells were lysed with [10mM Tris-HCl (pH 8.0), 10 mM NaCl, 3 mM MgCl<sub>2</sub>, 0.5% NP-40]. Nuclei were collected by centrifugation, resuspended in [1% SDS, 5 mmol/L EDTA, 50 mmol/L Tris-HCl (pH 8.0)] and sonicated to generate chromatin to an average length of ~100 to 500 bp. Next, samples in [1% Triton X-100, 2 mM EDTA, 20 mM Tris-HCl of pH 8.1, 150 mM NaCl], were immunoprecipitated overnight at 4°C with 4 µg ChIP-grade antibody. 20 µl of magnetic beads (Dynabeads M-280, Invitrogen) were used to purify immunocomplexes. Following purification, cross-links were reverted by incubation at 65°C for 6 h. Samples were purified with Qiagen kit. For ChIP re-ChIP analysis, DNA-protein complexes were eluted in 25 µL of TE buffer containing 10 mM DTT for 30 min at 37°C. Eluates were diluted 1:20 with ChIP Dilution buffer and used for second immunoprecipitation. Primers were as follows:

CDK4 agcaatgtcaagcgggtcac, acaggccgcaagctagagag;

CCNB1 gcttcactgctctccaggtg,  
 cactcactcccttccattg;  
 MRC1, ctgccagctgaaaagaact,  
 gttttccagccaccctcat;  
 STAT6, gatgtctgcaggcagagtgg,  
 tgcattggcttgcacaac;  
 PPARG, aagaaggaaaggagggaagg,  
 tgtgtgtttccaccctagc.

### Proximity Ligation Assay

Proximity ligation assays (PLA) were carried out using a PLA kit (Sigma) according to manufacturer's instructions. Prior to detection THP-1 cells were fixed with 4% PFA, washed and permeabilized with 1% Triton in PBS, blocked with supplied PLA blocking buffer and incubated with primary antibodies as indicated. Interactions were visualized using Duolink Brightfield detection reagent (Sigma). The PLA assay omitting one or both primary antibodies was used as a negative control.

### Immunofluorescence

Cells were fixed with 4% paraformaldehyde for 15 minutes at room temperature, washed with PBS and permeabilized with 1% Triton X-100 for 15 minutes then blocked in immunofluorescence buffer (PBS containing 2.5 mM EDTA, 1% BSA) for 1 hour. Cells were then incubated with primary antibody, 1:300 in PBS containing 2.5 mM EDTA, 1% BSA, 0.1% Triton X-100 overnight at 4°C. After washing with PBS, coverslips were incubated with Alexa Fluor -conjugated secondary antibody (1:500) in 0.1 µg/ml DAPI for 1 hour in the dark at RT. Coverslips were washed and mounted with FluorSave Reagent (Calbiochem, La Jolla, CA). Slides were observed in a Nikon Eclipse 800 upright epifluorescence microscope (Nikon Instruments, Melville, NY). Images were acquired using a Nikon CoolSNAP camera.

### Western Blots

Protein extracts (15 µg) were subjected to 10% SDS-polyacrylamide gel electrophoresis

(SDS-PAGE), electrophoretically transferred to nitrocellulose membranes (Amersham Hybond ECL, GE Healthcare), and blocked in 3% BSA/PBS at RT for 1 hour. Primary antibodies were incubated overnight at manufacturer recommended concentrations. Immunoblots were detected with the ECL Plus Western Blotting Detection System (Amersham Biosciences, Piscataway, NJ) or using near-infrared fluorescence with the ODYSSEY Fc, Dual-Mode Imaging system (Li-COR). Expression levels were evaluated by quantification of relative density of each band normalized to that of the corresponding β-actin or GAPDH band density.

### ELISA

Modified Enzyme-linked immunosorbent assays (ELISAs) were carried out as following. Plastic 96 well microtiter plates (Immuno Maxi Sorb, Nunc) were coated overnight with excess (0.5 µg) of first primary antibody. Unbound protein was washed with PBS. Wells were blocked for 1 h with 0.3 ml 3% BSA (Sigma, Cohn Fraction V, essentially fatty acid free) in PBS. After washing, samples containing the protein of interest (in 50 µl) were added, incubated for 2 h at room temperature and then washed with PBS. Second primary antibody (0.1 µg in 50 µl) was added, incubated for 1 h at room temperature, washed and then visualized by incubation with secondary antibody conjugated with horseradish peroxidase (Jackson Lab, Inc) in the presence of 3% BSA for 0.5 h, followed by reaction with ABTS (Sigma). The reaction was allowed to proceed for 20 min and then plates were quantitated spectrophotometrically at 410 nm.

### Immunohistochemistry

Immunostaining on formalin-fixed sections was performed by deparaffinization and rehydration, followed by antigen retrieval by heating in a pressure cooker (121°C) for 5 minutes in 10 mM sodium citrate, pH 6.0.



Peroxidase activity was blocked by incubation in 3% hydrogen peroxide for 10 minutes. Sections were rinsed three times in PBS/PBS-T (0.1% Tween-20) and incubated in Dako Protein Block (Dako) at room temperature for 1 hour. After removal of blocking solution, slides were placed into a humidified chamber and incubated overnight with an antibody, diluted 1:300 in Dako Protein Block at 4°C. Antigen was detected using the SignalStain Boost IHC detection reagent (catalogue # 8114; Cell Signaling Technology, Beverly, MA), developed with diaminobenzidine (Dako, Carpinteria, CA), counterstained with hematoxylin (Sigma-Aldrich), and mounted. Signal intensity was analyzed by Aperio

ImageScope 12.1, intensity for hepatocytes and non-parenchymal cells was calculated using nuclear size cut-off: for hepatocytes - nuclear area  $>10\mu\text{m}^2$ , non-parenchymal cells - nuclear area  $5-10\mu\text{m}^2$ .

### Statistics

Results are expressed as mean  $\pm$  SD. The Student t test, paired t test, Pearson's correlation, or one-way ANOVA with Bonferroni post hoc test was used for statistical analyses. p value  $< 0.05$  was considered significant.

### Acknowledgements

This study was supported by grants AA012863 from the National Institute on Alcoholism and Alcohol Abuse, COBRE grant NCRR/NIH P20 RR021940 and Pinnacle Research Award 2016 from AASLD. The human liver specimens used in this study were derived from samples provided by the University of Kansas Liver Center Tissue Bank. We thank Drs. Jameson Forster, Tim Schmitt, and Bashar Abdulkarim for their assistance in obtaining these specimens.

**Conflict of interest:** The authors declare that they have no conflicts of interest with the contents of this article.

### Authorship Contributions

Contribution: I.T. and S.A.W. designed the research, analyzed the results, and wrote the manuscript; I.T and J.Z. performed the experiments; IT produced the figures, S.K. B.B., B.R., collected human specimens. All authors analyzed the results and approved the final version of the manuscript.

## References

1. Bedford, M. T., and Richard, S. (2005) Arginine methylation an emerging regulator of protein function. *Mol Cell* **18**, 263-272
2. Tang, J., Frankel, A., Cook, R. J., Kim, S., Paik, W. K., Williams, K. R., Clarke, S., and Herschman, H. R. (2000) PRMT1 is the predominant type I protein arginine methyltransferase in mammalian cells. *The Journal of biological chemistry* **275**, 7723-7730
3. Gary, J. D., and Clarke, S. (1998) RNA and protein interactions modulated by protein arginine methylation. *Progress in nucleic acid research and molecular biology* **61**, 65-131
4. Bedford, M. T., and Clarke, S. G. (2009) Protein arginine methylation in mammals: who, what, and why. *Mol Cell* **33**, 1-13
5. Adhikary, S., and Eilers, M. (2005) Transcriptional regulation and transformation by Myc proteins. *Nature reviews. Molecular cell biology* **6**, 635-645
6. Levens, D. L. (2003) Reconstructing MYC. *Genes & development* **17**, 1071-1077
7. Adhikary, S., Marinoni, F., Hock, A., Hulleman, E., Popov, N., Beier, R., Bernard, S., Quarto, M., Capra, M., Goettig, S., Kogel, U., Scheffner, M., Helin, K., and Eilers, M. (2005) The ubiquitin ligase HectH9 regulates transcriptional activation by Myc and is essential for tumor cell proliferation. *Cell* **123**, 409-421
8. Baena, E., Ortiz, M., Martinez, A. C., and de Alboran, I. M. (2007) c-Myc is essential for hematopoietic stem cell differentiation and regulates Lin(-)Sca-1(+)c-Kit(-) cell generation through p21. *Experimental hematology* **35**, 1333-1343
9. Guo, Y., Niu, C., Breslin, P., Tang, M., Zhang, S., Wei, W., Kini, A. R., Paner, G. P., Alkan, S., Morris, S. W., Diaz, M., Stiff, P. J., and Zhang, J. (2009) c-Myc-mediated control of cell fate in megakaryocyte-erythrocyte progenitors. *Blood* **114**, 2097-2106
10. Pello, O. M., De Pizzol, M., Mirolo, M., Soucek, L., Zammataro, L., Amabile, A., Doni, A., Nebuloni, M., Swigart, L. B., Evan, G. I., Mantovani, A., and Locati, M. (2012) Role of c-MYC in alternative activation of human macrophages and tumor-associated macrophage biology. *Blood* **119**, 411-421
11. Tikhanovich, I., Kuravi, S., Artigues, A., Villar, M. T., Dorko, K., Nawabi, A., Roberts, B., and Weinman, S. A. (2015) Dynamic Arginine Methylation of Tumor Necrosis Factor (TNF) Receptor-associated Factor 6 Regulates Toll-like Receptor Signaling. *The Journal of biological chemistry* **290**, 22236-22249
12. Tikhanovich, I., Zhao, J., Olson, J., Adams, A., Taylor, R., Bridges, B., Marshall, L., Roberts, B., and Weinman, S. A. (2017) Protein Arginine Methyltransferase 1 modulates innate immune responses through regulation of peroxisome proliferator-activated receptor gamma-dependent macrophage differentiation. *The Journal of biological chemistry*
13. Croasdell, A., Duffney, P. F., Kim, N., Lacy, S. H., Sime, P. J., and Phipps, R. P. (2015) PPARgamma and the Innate Immune System Mediate the Resolution of Inflammation. *PPAR research* **2015**, 549691
14. Lefevre, L., Authier, H., Stein, S., Majorel, C., Couderc, B., Dardenne, C., Eddine, M. A., Meunier, E., Bernad, J., Valentin, A., Pipy, B., Schoonjans, K., and Coste, A. (2015) LRH-1 mediates anti-inflammatory and antifungal phenotype of IL-13-activated macrophages through the PPARgamma ligand synthesis. *Nature communications* **6**, 6801
15. Odegaard, J. I., Ricardo-Gonzalez, R. R., Goforth, M. H., Morel, C. R., Subramanian, V., Mukundan, L., Red Eagle, A., Vats, D., Brombacher, F., Ferrante, A. W., and Chawla, A. (2007) Macrophage-specific PPARgamma controls alternative activation and improves insulin resistance. *Nature* **447**, 1116-1120

16. Szanto, A., Balint, B. L., Nagy, Z. S., Barta, E., Dezso, B., Pap, A., Szeles, L., Poliska, S., Oros, M., Evans, R. M., Barak, Y., Schwabe, J., and Nagy, L. (2010) STAT6 transcription factor is a facilitator of the nuclear receptor PPARgamma-regulated gene expression in macrophages and dendritic cells. *Immunity* **33**, 699-712
17. Zingarelli, B., and Cook, J. A. (2005) Peroxisome proliferator-activated receptor-gamma is a new therapeutic target in sepsis and inflammation. *Shock* **23**, 393-399
18. Barrero, M. J., and Malik, S. (2006) Two functional modes of a nuclear receptor-recruited arginine methyltransferase in transcriptional activation. *Molecular cell* **24**, 233-243
19. An, W., Kim, J., and Roeder, R. G. (2004) Ordered cooperative functions of PRMT1, p300, and CARM1 in transcriptional activation by p53. *Cell* **117**, 735-748
20. Yang, Y., McBride, K. M., Hensley, S., Lu, Y., Chedin, F., and Bedford, M. T. (2014) Arginine methylation facilitates the recruitment of TOP3B to chromatin to prevent R loop accumulation. *Molecular cell* **53**, 484-497
21. Eberhardt, A., Hansen, J. N., Koster, J., Lotta, L. T., Jr., Wang, S., Livingstone, E., Qian, K., Valentijn, L. J., Zheng, Y. G., Schor, N. F., and Li, X. (2016) Protein arginine methyltransferase 1 is a novel regulator of MYCN in neuroblastoma. *Oncotarget* **7**, 63629-63639
22. Cho, M. H., Park, J. H., Choi, H. J., Park, M. K., Won, H. Y., Park, Y. J., Lee, C. H., Oh, S. H., Song, Y. S., Kim, H. S., Oh, Y. H., Lee, J. Y., and Kong, G. (2015) DOT1L cooperates with the c-Myc-p300 complex to epigenetically derepress CDH1 transcription factors in breast cancer progression. *Nature communications* **6**, 7821
23. Borzio, M., Salerno, F., Piantoni, L., Cazzaniga, M., Angeli, P., Bissoli, F., Boccia, S., Colloredo-Mels, G., Corigliano, P., Fornaciari, G., Marengo, G., Pistara, R., Salvagnini, M., and Sangiovanni, A. (2001) Bacterial infection in patients with advanced cirrhosis: a multicentre prospective study. *Digestive and liver disease : official journal of the Italian Society of Gastroenterology and the Italian Association for the Study of the Liver* **33**, 41-48
24. Uribealago, I., Benitah, S. A., and Di Croce, L. (2012) From oncogene to tumor suppressor: the dual role of Myc in leukemia. *Cell cycle* **11**, 1757-1764
25. Hassa, P. O., Covic, M., Bedford, M. T., and Hottiger, M. O. (2008) Protein arginine methyltransferase 1 coactivates NF-kappaB-dependent gene expression synergistically with CARM1 and PARP1. *Journal of molecular biology* **377**, 668-678
26. Tikhanovich, I., Olson, J. C., Taylor, R., Bridges, B., Dorko, K., Roberts, B. R., and Weinman, S. A. (2015) Impaired TRAF6 methylation and TLR responses in liver tissue and circulating monocytes from patients with spontaneous bacterial peritonitis. *Hepatology* **62**, 846a-846a
27. Ambade, A., Satishchandran, A., Saha, B., Gyongyosi, B., Lowe, P., Kodys, K., Catalano, D., and Szabo, G. (2016) Hepatocellular carcinoma is accelerated by NASH involving M2 macrophage polarization mediated by hif-1alpha-induced IL-10. *Oncoimmunology* **5**, e1221557
28. Cui, Y. L., Li, H. K., Zhou, H. Y., Zhang, T., and Li, Q. (2013) Correlations of tumor-associated macrophage subtypes with liver metastases of colorectal cancer. *Asian Pacific journal of cancer prevention : APJCP* **14**, 1003-1007
29. Shirabe, K., Mano, Y., Muto, J., Matono, R., Motomura, T., Toshima, T., Takeishi, K., Uchiyama, H., Yoshizumi, T., Taketomi, A., Morita, M., Tsujitani, S., Sakaguchi, Y., and Maehara, Y. (2012) Role of tumor-associated macrophages in the progression of hepatocellular carcinoma. *Surgery today* **42**, 1-7
30. Yeung, O. W., Lo, C. M., Ling, C. C., Qi, X., Geng, W., Li, C. X., Ng, K. T., Forbes, S. J., Guan, X. Y., Poon, R. T., Fan, S. T., and Man, K. (2015) Alternatively activated (M2) macrophages promote tumour growth and invasiveness in hepatocellular carcinoma. *Journal of hepatology* **62**, 607-616
31. Davies, J. Q., and Gordon, S. (2005) Isolation and culture of murine macrophages. *Methods in molecular biology* **290**, 91-103

32. Li, Z., Zhao, J., Tikhanovich, I., Kuravi, S., Helzberg, J., Dorko, K., Roberts, B., Kumer, S., and Weinman, S. A. (2016) Serine 574 phosphorylation alters transcriptional programming of FOXO3 by selectively enhancing apoptotic gene expression. *Cell death and differentiation* **23**, 583-595



## Figure legends

**Figure 1. Arginine methylation regulates c-Myc cofactor binding.** **A.** Representative images of c-Myc immunofluorescence analysis in untreated or AMI-1 treated (50  $\mu$ M for 16h) THP1 cells. **B.** Western blot analysis of immunoprecipitation using anti-c-Myc antibody or IgG as a negative control in untreated or AMI-1 treated (10  $\mu$ M and 50  $\mu$ M for 16h) THP-1 cells. Lower panels show the densitometry quantification of p300/Max/HDAC1 signal from three independent IP experiments. Data are presented as mean  $\pm$  SD.  $^{**}p < 0.01$ . **C.** Western blot analysis of immunoprecipitation using anti-p300 antibody or IgG as a negative control in untreated or AMI-1 treated (50  $\mu$ M for 16h) THP-1 cells. **D.** Representative images of proximity ligation assays (PLA) in THP-1 cells. c-Myc interaction with PRMT1 was detected using anti-PRMT1 and anti-c-Myc antibodies. Negative control – signal in the absence of primary antibodies. **E.** Representative images of proximity ligation assays (PLA) for c-Myc interaction with p300, Max or Miz1 in THP-1 cells untreated or treated with 50  $\mu$ M AMI-1 was detected using anti-p300, anti-Max or anti-Miz1 and anti-c-Myc. Average number of PLA positive THP-1 cells is shown for three independent experiments (right). Data are presented as mean  $\pm$  SD.  $^{**}p < 0.01$ . **F.** Western blot analysis of immunoprecipitation using anti-c-Myc antibody or IgG as a negative control in wild type and PRMT1 knockout macrophages.

**Figure 2. c-Myc is arginine methylated.** **A.** Sites of c-Myc arginine methylation. Mass spectrometry analysis of c-Myc purified from THP-1 cells. MS-MS spectra of methylated and corresponding unmethylated peptides for each site with highest A-scores. **B.** Schematic image of c-Myc domain structure, MYC N, N terminal transactivation domain, HLH, helix-loop-helix DNA binding domain, LZ, leucine zipper Max dimerization domain. Image shows the position of methylated arginines relative to known co-factor binding overlapping with methylated arginine sites. **C.** Relative p300/c-Myc binding was measured by ELISA as described in Methods. Relative p300/c-Myc binding is plotted against PRMT1 expression in individual patient-derived peripheral blood monocyte samples.

**Figure 3. Arginine methylation effect on c-Myc promoter binding and co-factor recruitment.** **A, C.** Chromatin immunoprecipitation (ChIP) using anti-c-Myc, anti-p300, anti-HDAC1, anti-H3K27ac antibody or IgG as a negative control in untreated or AMI-1 treated THP-1 cells. Data are presented as mean percent of input  $\pm$  SD.  $n=3-5$ .  $^{*}p < 0.05$ ,  $^{**}p < 0.01$ . **B, D.** c-Myc ChIP followed by p300 or HDAC1 re-ChIP using anti-p300 or anti-HDAC1 antibody or IgG as a negative control in untreated or AMI-1 treated THP-1 cells. Data are presented as mean percent of input  $\pm$  SD.  $n=3-5$ .  $^{*}p < 0.05$ ,  $^{**}p < 0.01$ .

**Figure 4. Arginine methylation regulates c-Myc transcriptional activation activity.** **A.** c-Myc downregulates PRMT1 gene expression. Western blot analysis of PRMT1 protein levels in THP-1 cells expressing c-Myc (left). Relative mRNA of PRMT1 in THP-1 cells expressing wild type c-Myc (right). Data are presented as mean  $\pm$  SD.  $^{**}p < 0.01$   $n \geq 3$ . **B.** Relative mRNA of Cyclin B1, CDK4, PPAR $\gamma$ , STAT6 and CD209 in untreated or AMI-1 treated THP-1 cells expressing wild type c-Myc and wild type PRMT1(P1) where indicated. Data are presented as mean  $\pm$  SD.  $^{*}p < 0.05$ ,  $^{**}p < 0.01$  compared to c-Myc only,  $^{+}p < 0.05$ ,  $^{++}p < 0.01$  compared to untreated.  $n \geq 3$ . **C.** Representative images of M2 marker expression (MRC1 or CD206) by immunofluorescence analysis in untreated or AMI-1 treated THP-1 macrophages expressing wild type c-Myc and wild type PRMT1 where indicated. Average fluorescence intensity is shown on the right. Data are presented as mean  $\pm$  SD.  $^{**}p < 0.01$   $n=3$ .

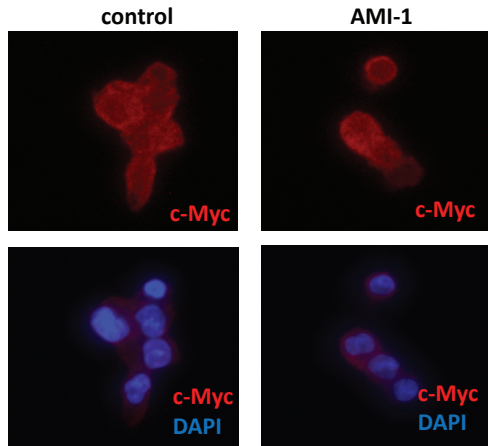
**Figure 5. R299K\_R346K c-Myc mutant has impaired p300 binding and transcriptional activation.** **A.** PLA detection of c-Myc wild type or mutants binding to Max, HDAC1 and p300. **B.** ChIP assay using anti-Flag antibody or IgG as a negative control (top). Flag ChIP followed by p300 re-ChIP (bottom). Data are presented as mean percent of input  $\pm$  SD. \* $p < 0.05$ , \*\* $p < 0.01$  compared to IgG.  $n=3$ . **C.** Relative mRNA of Cyclin B1 and CDK4 in untreated or AMI-1 treated THP-1 cells expressing wild type or mutant c-Myc and wild type PRMT1 where indicated. Expression is normalized to no c-Myc overexpression. Data are presented as mean  $\pm$  SD. \* $p < 0.05$ , \*\* $p < 0.01$  compared to c-Myc wild type.  $n=3$ .

**Figure 6. PRMT1 is downregulated in livers from patients with decompensated cirrhosis.** **A.** Relative staining intensity of PRMT1 staining in hepatocytes and non-parenchymal cells measured by Aperio ImageScope in liver tissue sections of patients with or without history of spontaneous bacterial peritonitis (SBP).  $n = 5$  in each group. \* $p < 0.05$ . **B.** Examples of liver tissue sections with or without history of SBP stained for PRMT1 protein and MRC1 (CD206). **C.** Average number of CD206 positive cells per field in liver tissue sections of patients with or without history of SBP as in A. **D.** Representative images of liver tissue sections stained with PRMT1 and CD206 or c-Myc and CD206; arrows indicate double positive cells. **E.** Correlation between PRMT1 staining intensity and average number of CD206 positive cells per field (left). Correlation between average number of c-Myc positive cells and average number of CD206 positive cells (right). **F.** Number of CD206 positive cells in sections with low PRMT1 and c-Myc, low PRMT1 and high c-Myc, high PRMT1 and low c-Myc, or high PRMT1 and c-Myc (high high). Data are presented as mean  $\pm$  SD. \* $p < 0.05$ , \*\* $p < 0.01$ , \*\*\* $p < 0.001$ .

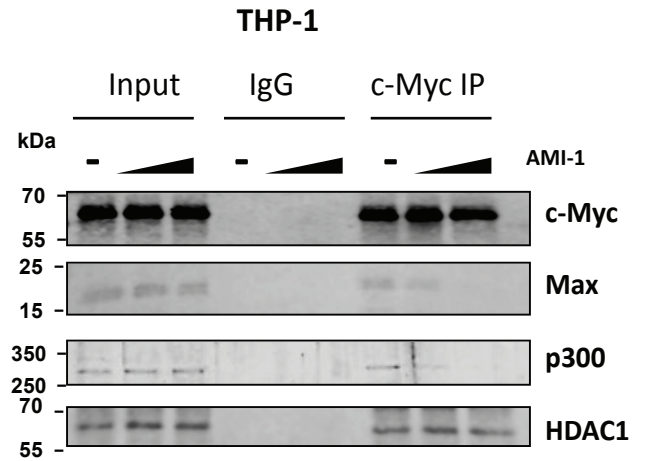
**Figure 7. A model of c-Myc regulation by arginine methylation.** Equilibrium between c-Myc-p300 and c-Myc-HDAC1 complexes is regulated by PRMT1 activity. In the presence of PRMT1 c-Myc is arginine methylated on R299 and R346 and can efficiently bind p300. When PRMT1 activity is inhibited, c-Myc can no longer bind p300 and binds HDAC1 instead. In patients with cirrhosis and SBP PRMT1 expression is low. That decreases c-Myc activity and lowers number of M2 anti-inflammatory macrophages in the liver.

# Figure 1

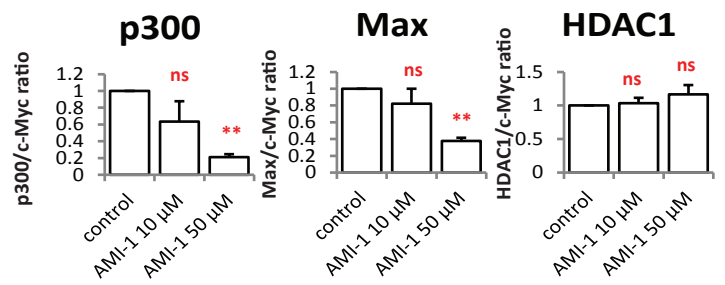
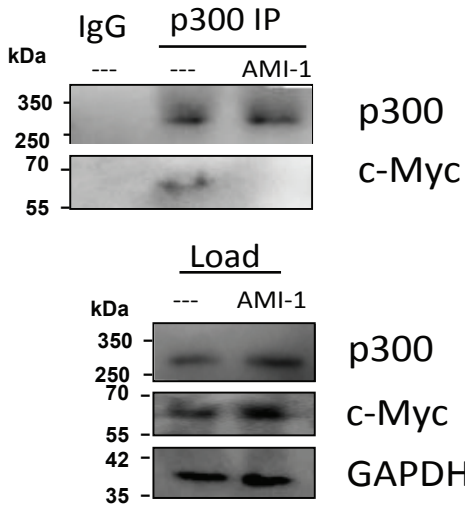
**A**



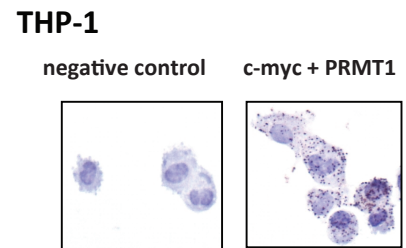
**B**



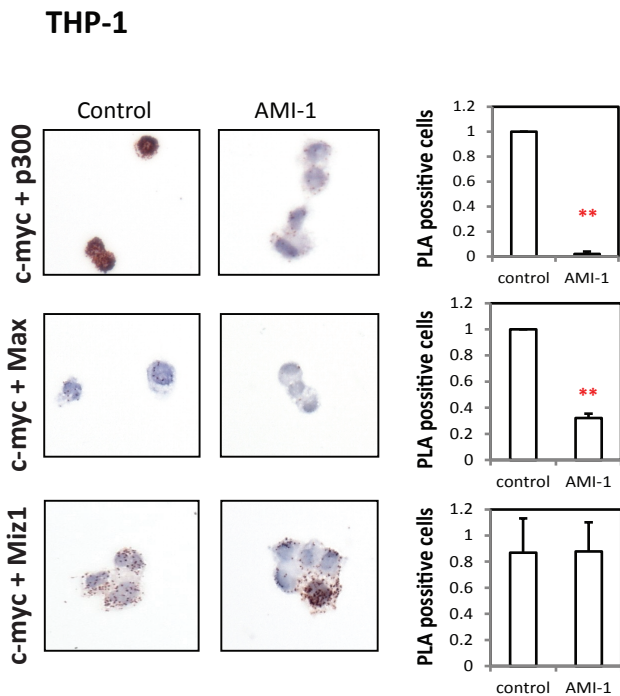
**C**



**D**



**E**



**F**

**primary macrophages**

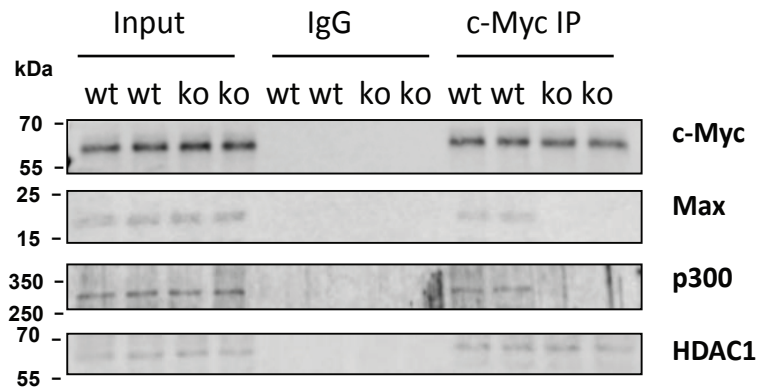
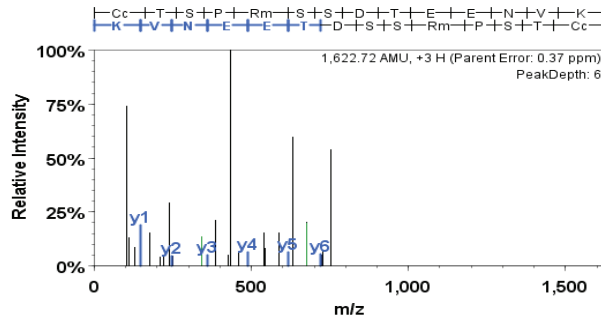


# Figure 2

A

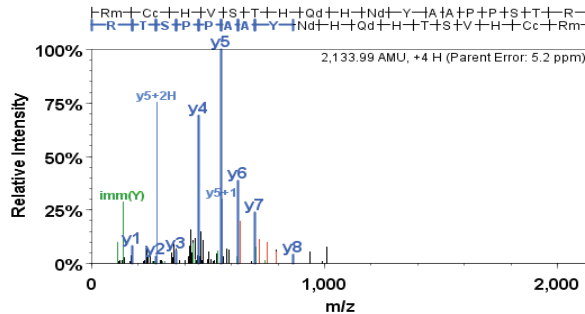
R346me

cTSPrSSDTEENVK 100% 1,000.00(A-score)



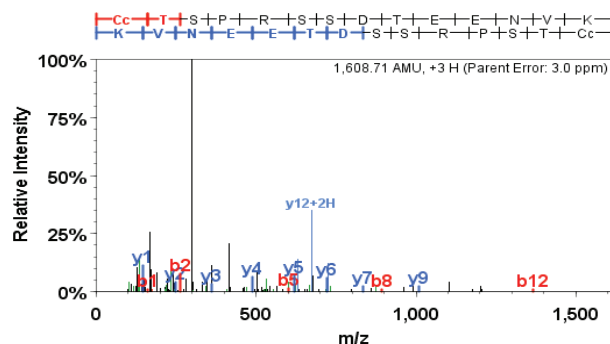
R299me

rcHVSTHqHnYAAPPSTR 100% 223.43 (A-score)



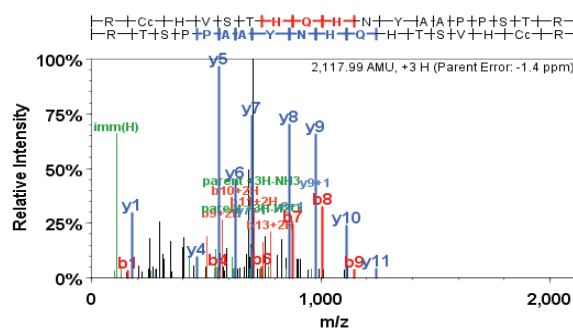
R346

cTSPRSDTEENVK

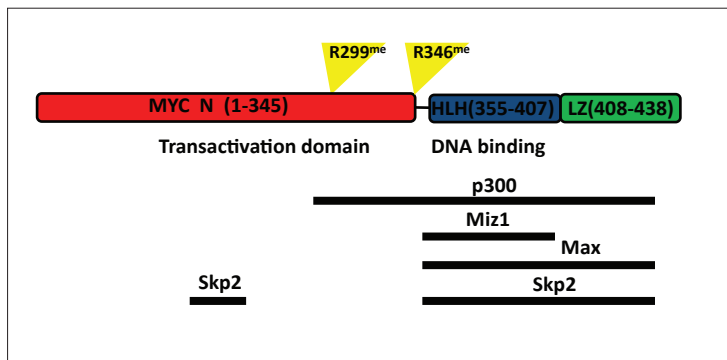


R299

RcHVSTHQHNYAAPPSTR



B



C

p300 - c-Myc binding in monocytes

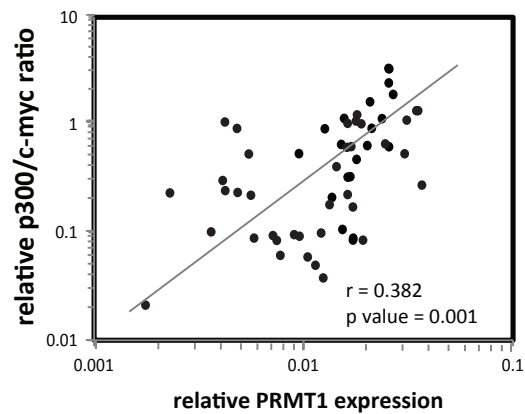
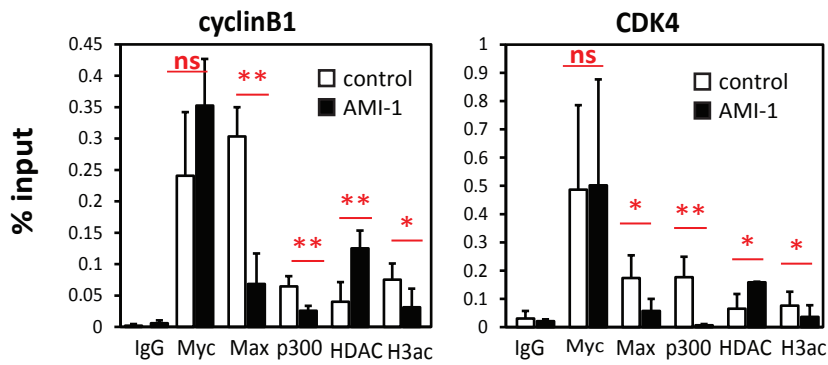




# Figure 3

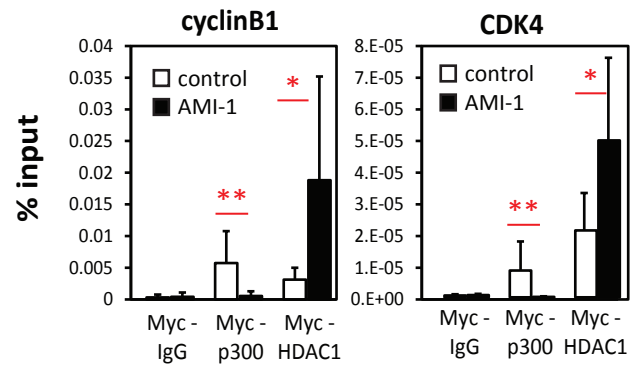
**A**

ChIP



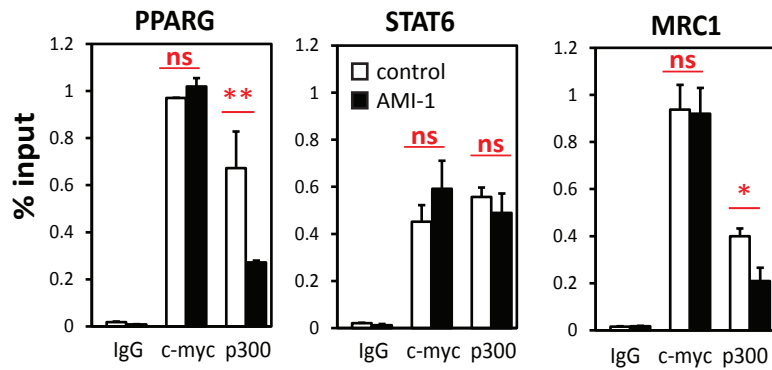
**B**

ChIP-re-ChIP



**C**

ChIP



**D**

ChIP-re-ChIP

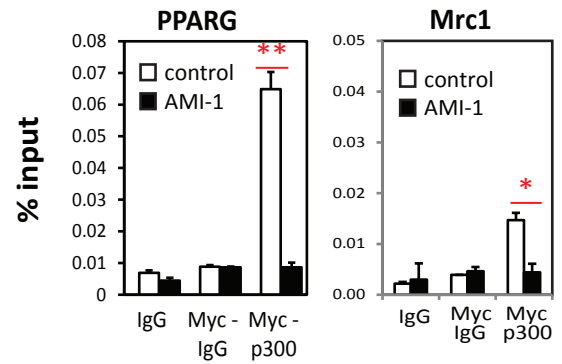
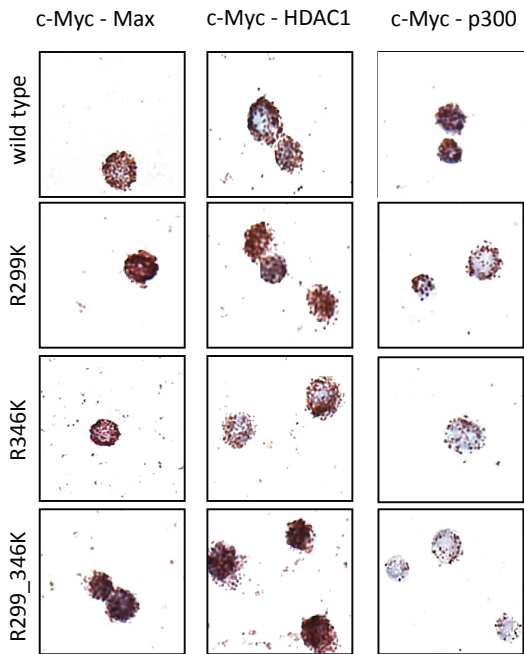


## Figure 4

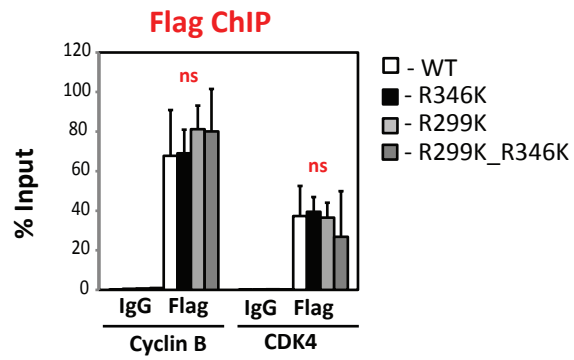


# Figure 5

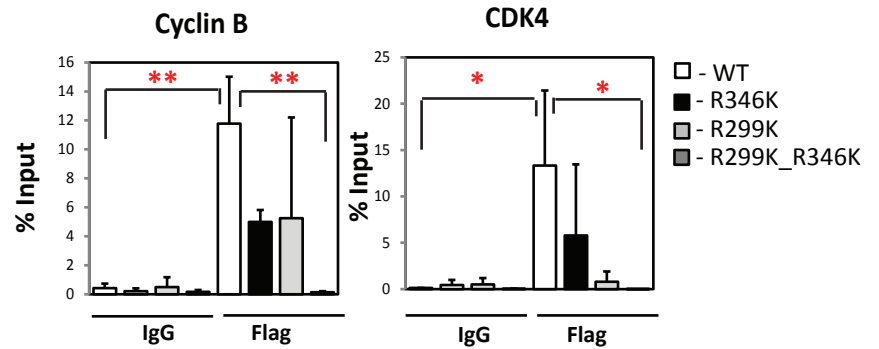
**A**



**B**



**Flag ChIP - p300 re-ChIP**



**C**

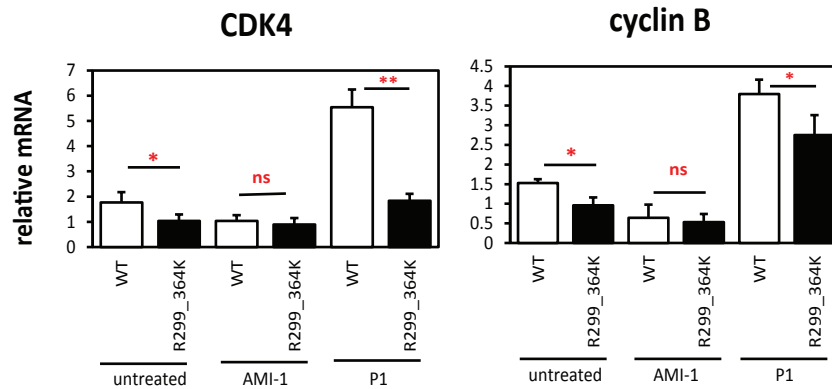
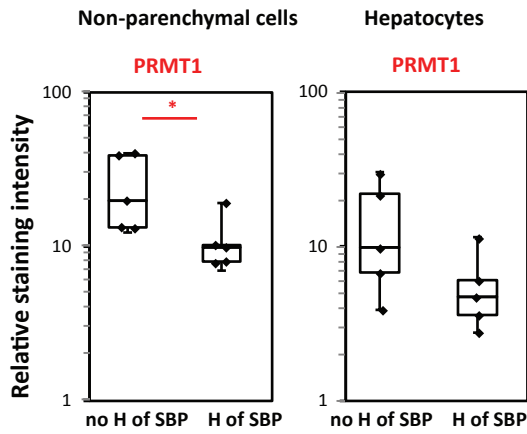
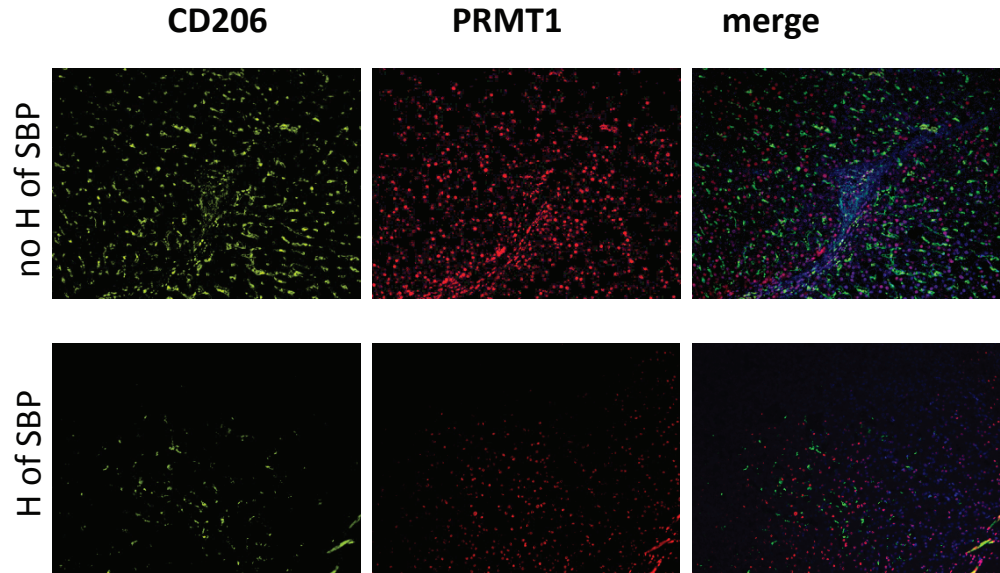


# Figure 6

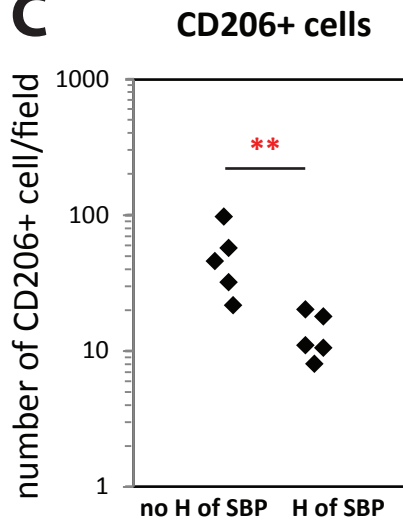
**A**



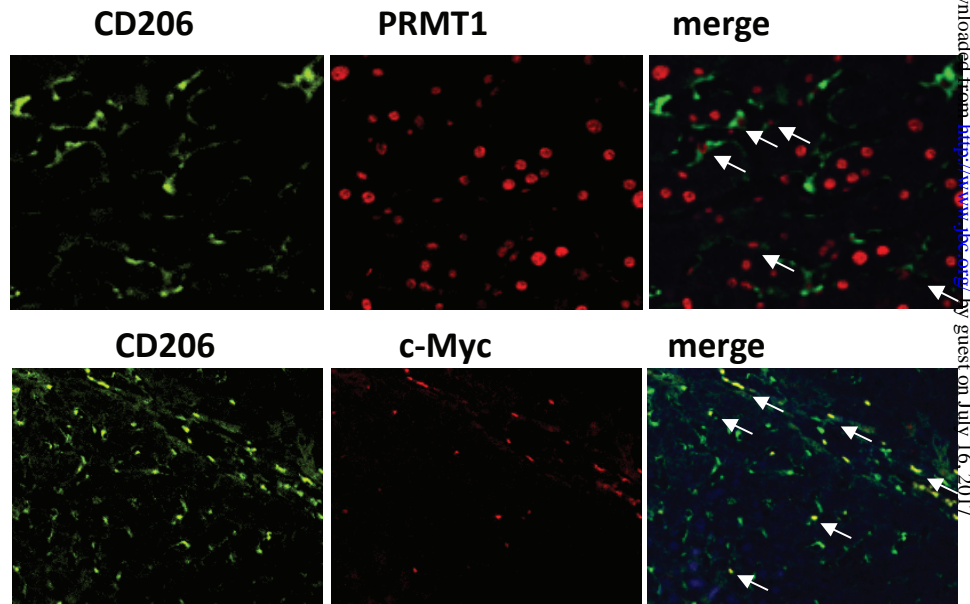
**B**



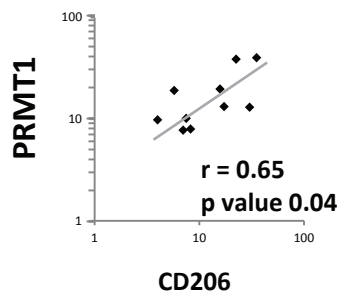
**C**



**D**



**E**



**F**

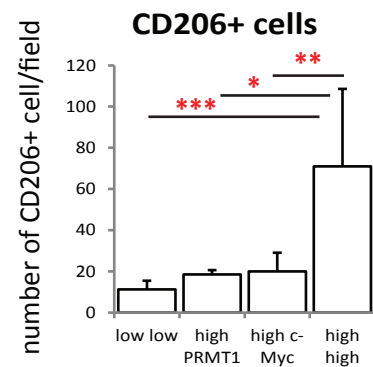
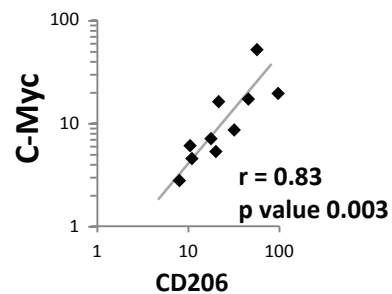
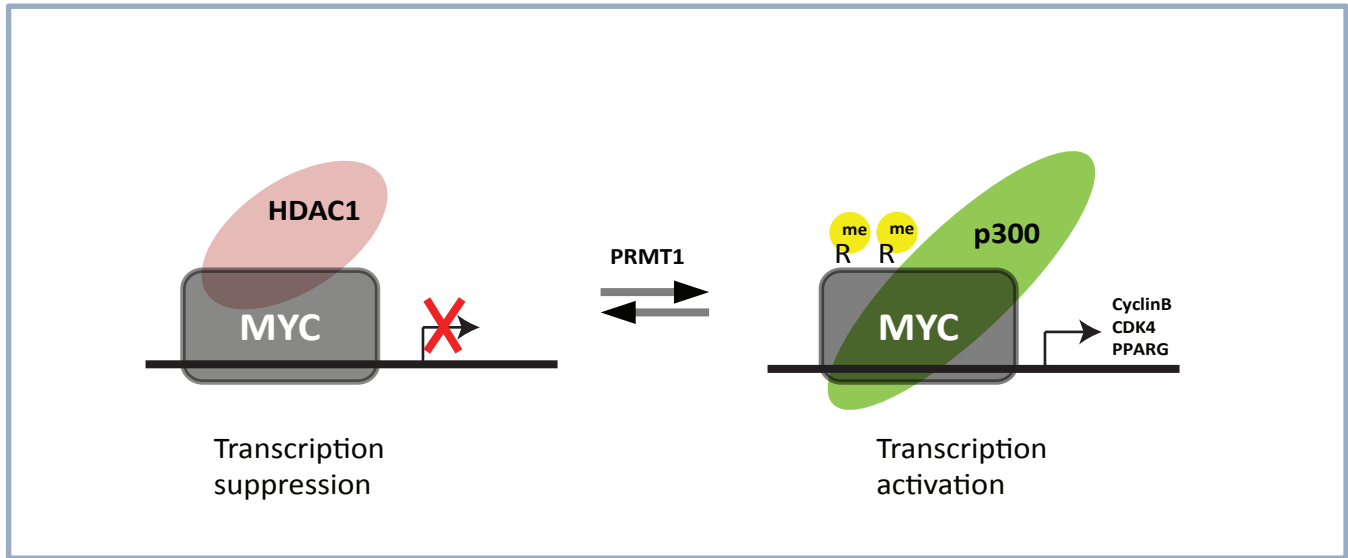




# Figure 7



**Arginine methylation regulates c-Myc-dependent transcription by altering promoter recruitment of the acetyltransferase p300**

Irina Tikhanovich, Jie Zhao, Brian Bridges, Sean Kumer, Ben Roberts and Steven A Weinman

*J. Biol. Chem.* published online June 26, 2017

---

Access the most updated version of this article at doi: [10.1074/jbc.M117.797928](https://doi.org/10.1074/jbc.M117.797928)

Alerts:

- [When this article is cited](#)
- [When a correction for this article is posted](#)

[Click here](#) to choose from all of JBC's e-mail alerts

This article cites 0 references, 0 of which can be accessed free at  
<http://www.jbc.org/content/early/2017/06/26/jbc.M117.797928.full.html#ref-list-1>